Microfluidic chemical processing with on-chip washing by deterministic lateral displacement arrays with separator walls

Yu Chen,[1,2] Joseph D'Silva,[1,2] Robert H. Austin,[1,3] and James C. Sturm[1,2]
[1]*Princeton Institute for Science and Technology of Materials (PRISM), Princeton, New Jersey 08544, USA*
[2]*Department of Electrical Engineering, Princeton University, Princeton, New Jersey 08544, USA*
[3]*Department of Physics, Princeton University, Princeton, New Jersey 08544, USA*

(Received 6 July 2015; accepted 31 August 2015; published online 9 September 2015)

We describe a microfluidic device for on-chip chemical processing, such as staining, and subsequent washing of cells. The paper introduces "separator walls" to increase the on-chip incubation time and to improve the quality of washing. Cells of interest are concentrated into a treatment stream of chemical reagents at the first separator wall for extended on-chip incubation without causing excess contamination at the output due to diffusion of the unreacted treatment chemicals, and then are directed to the washing stream before final collections. The second separator wall further reduces the output contamination from diffusion to the washing stream. With this approach, we demonstrate on-chip leukocyte staining with Rhodamine 6G and washing. The results suggest that other conventional biological and analytical processes could be replaced by the proposed device. © *2015 AIP Publishing LLC*.
[http://dx.doi.org/10.1063/1.4930863]

INTRODUCTION

Many preparation steps for the analysis of biological cells involve the chemical treatment of the cells (such as staining by monoclonal antibodies and a fixation/permeabilization step). These steps are typically followed by a "washing" step to remove the unbound labels or excess treatment chemicals from the treated cells, to yield treated and washed cells. Both the treatment and the washing usually require multiple manual steps, which may include pipetting, centrifugation, and re-suspension of a pellet after centrifugation. These labor-intensive steps will inevitably cause variations to the quality of prepared cells and the results of subsequential analysis or diagnosis.[1]

For more uniformly prepared samples, automated and integrated processing and preparation of cells are preferred. Some microfluidic devices can perform one of the cell preparation steps. McClain *et al*. have shown a microchannel for on-chip cell lysis using electric field.[2] Conventional centrifugation (and washing) are still needed before (and after) the on-chip cell lysis. Moreover, the distinctive structures of these devices often lead to difficulties in higher level integration. Nguyen *et al*. have presented a Polydimethylsiloxane (PDMS) microfluidic system for on-chip blood cell preparation and analysis,[3] which has a complicated design of multiple functional sections and needs accurate fluid controls to function correctly, limiting its practicality.

Other cell preparation and processing devices with simpler structures include a "centrifuge on-chip" device for cell preparation using simple rectangular shaped channels.[4] However, the underlying separation mechanism of on-chip vortices limits the cell capture efficiency to 20% and purity to 40%. Integrated microfluidic devices for chemical treatment with high cell capture efficiency are often limited by the diffusion of the treatment chemical. The diffusion of the treatment chemical will cause a contamination at the output by the treatment chemical and a decrease of the effective concentration of the treatment chemical. Usually, a high fluid velocity is required to avoid this diffusion. In one device, inertial lift force is utilized as the separation

 © 2015 AIP Publishing LLC

This article is copyrighted as indicated in the article. Reuse of AIP content is subject to the terms at: http://scitation.aip.org/termsconditions. Downloaded to IP: 128.112.141.27 On: Wed, 09 Sep 2015 13:48:43

mechanism to give very high cell capture efficiency.[5] The cells are directed into a sodium carbonate stream from a hematoxylin suspension buffer with an acetic acid stream as diffusion barrier to avoid the mixture of sodium carbonate and hematoxylin suspension buffer. However, the fluid velocity is ~0.6 m/s for a treatment chemical's diffusion constant of 10^{-9} m^2/s, requiring a separate on-chip or off-chip incubation.

Morton *et al.* have presented a method for on-chip cell processing in a continuous-flow microfluidic chip, in which deterministic lateral displacement (DLD) arrays are used to move target cells into and then out of a treatment chemical processing stream.[6] Again, high fluid velocities are required to avoid the diffusion of the treatment chemical. However, the device design and high cell capture efficiency and purity[7,8] make the proposed device attractive. Inspired by this work, in this paper, we demonstrate an on-chip cell processing and preparation approach to achieve both long incubation time and low contamination of the excess treatment chemical using "wall-separated" DLD arrays. We demonstrate a three-input (sample stream, treatment stream, and washing stream) microfluidic device for on-chip leukocyte staining and washing using Rhodamine 6G (R6G) with little output contamination. R6G molecules are commonly used staining dye in biological analysis[9] and have diffusion constant of 4×10^{-10} m^2/s in water, close to that of ethanol, methanol, and 1–2 orders of magnitude higher than that of monoclonal antibodies,[10] all commonly used in chemical and biological treatment.

MATERIALS AND METHODS

Microfluidic device design

Fig. 1(a) demonstrates the proposed "wall-separated" DLD array design. The input consists of three streams: a sample stream (diluted blood in our experiments), a treatment stream (such as staining chemicals), and a washing stream (such as bovine serum albumin (BSA) buffer). The output consists of two streams: the product of treated and washed cells, and waste. In the central region, there is a DLD array consisting of an array of posts slightly tilted by a small angle ϵ from the average flow direction imposed by the walls. Cells smaller than a critical size D_c (small cell in Fig. 1(b)) will follow the stream waving around the posts in an average horizontal direction as pointed out by the black arrow. Cells larger than this critical size (target cell

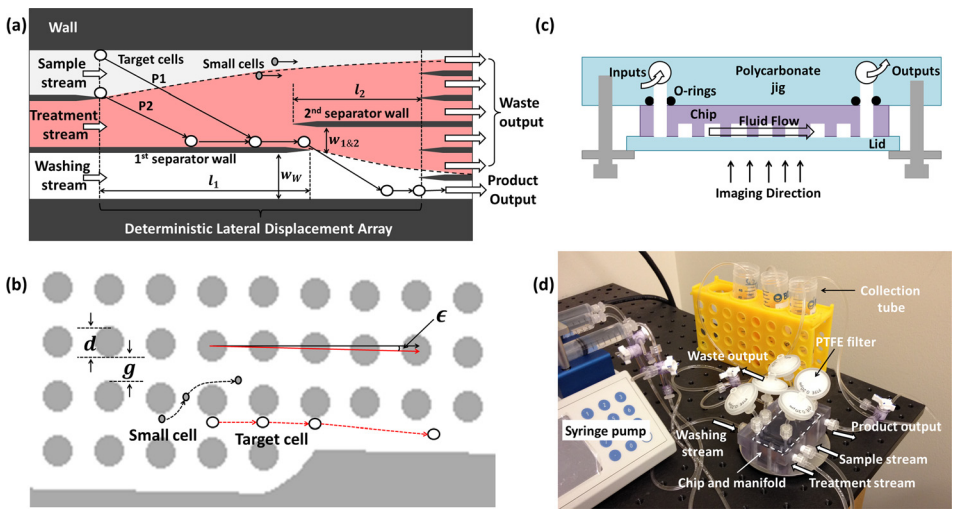

FIG. 1. (a) The schematic of the wall-separated DLD array design for on-chip cell processing and washing. Target cells (following paths P1 and P2) are processed and washed in a continuous fluidic flow. Separator walls reduce the diffusion of the treatment chemical, indicated by red shading, to minimize the contamination in the product output. (b) The schematic of detailed DLD array design ($d = 18\,\mu$ m, $g = 18\,\mu$ m, and $\epsilon = 1.36°$), and cell motion in this DLD array. Cells smaller than a critical size will follow the stream line in an average straight direction (small cell, black arrow), while cells larger than the critical size will bump at posts following the tilted axis of the array (target cell, red arrow). (c) Schematic of the manifold setup and (d) experimental setup for on-chip cell processing.

This article is copyrighted as indicated in the article. Reuse of AIP content is subject to the terms at: http://scitation.aip.org/termsconditions. Downloaded to IP: 128.112.141.27 On: Wed, 09 Sep 2015 13:48:43

in Fig. 1(b)) will follow the axis of the post array, "bumping" off of the post in each column as pointed out by the red arrow.[11] The large cells move into the treatment stream to be treated and then out of the treatment stream to be washed and collected as product output (Fig. 1(a)).[6] The critical size is determined by the geometry of the DLD array.[11] In this work, as shown in Fig. 1(b), with $d = 18\,\mu$m diameter spherical posts and $g = 18\,\mu$m gaps between the posts, and $\epsilon = 1.36^{\circ}$, the critical size (D_c) is about 6 μm. The wall edges of the DLD array are designed according to Inglis' guidelines, with a periodically varying gap between wall and posts, but which is always larger than the cell size to avoid clogging.[12]

The innovations of this paper are the "separator walls." A first wall prevents any chemical diffusion (indicated by red shading in Fig. 1(a)) towards the output, while the cells are being incubated. The target cells or particles are concentrated at the first separator wall of length $l_1 = 2$ cm, and then they are directed into the washing stream. After the first separator wall, target cells will be bumped by the DLD array and driven into and across the washing stream to be collected. The treatment stream is now free to diffuse to the product output, and the diffusion into the chip output is constrained only to this region, while the conventional DLD array has diffusion to the product output occurring all across the whole array. The treatment chemical has shorter diffusion time in the "wall-separated" DLD array than that in conventional DLD array. The diffusion in this last region can again be suppressed by adding a second separator wall, of length $l_2 = 1$ cm in the current design. The second separator wall will reduce a portion of the chemical reagents from being able to diffuse towards the output channel. The gap ($w_{1\&2}$) between the first and second separator walls is 90 μm, which should be as small as possible to avoid treatment chemical reaching to the washing stream, but should be larger enough to avoid the clogging of target cells.

Device fabrication and operation

Devices with and without separator walls were fabricated in silicon wafers using standard microfabrication techniques. Etching masks were formed on the silicon wafers using single-layer photolithography (Karl Suss, MA6) with AZ 4330 photoresist (AZ Electronic Materials, USA) and AZ 300 MIF developer. Samples were then anisotropically etched to 120 μm deep using a Samco RIE800iPB for Deep Reactive Ion Etching (DRIE). Inlets and outlets are through-wafer holes created by sandblasting using 50 μm diameter aluminium oxide particles (PrepStart, Danville Engineering, USA). The devices were sealed with 3M 9795R polyolefin sealing tape with a backplane glass coverslip in the bottom ("Lid" in Fig. 1(c)). The devices were mounted to a polycarbonate jig (Fig. 1(c)) connected to an external syringe pump (Fusion 400, Chemyx, USA). Then, 0.2 μm Polytetrafluoroethylene (PTFE) filters were applied to the jig to allow air to be pushed out of the manifold. Finally, a stainless steel metal plate with a window for microscopic observation was used to hold the devices and the polycarbonate jig.

An inverted microscope (Nikon Eclipse Ti) was used to image the distribution of fluorescent R6G and labeled cells in the devices, with high pressure mercury lamp as an excitation source with a matching fluorescence filter set (TRITC, 532–556 nm excitation and 570–613 nm emission). Images and movies were recorded using a CoolSNAP ES2 CCD camera and NIS-Elements software.

Fig. 1(d) shows the entire syringe pump and microfluidic system. The system and tubing was first rinsed and wet with degassed 0.2% Pluronic F108 surfactant in deionized water and then the running buffer (see later). Next, the sample solution as the sample input stream, staining solution as the treatment input stream, and running buffer as the washing input stream were loaded into the syringe pump as device inputs and driven through the microfluidic system to run experiments. The syringe pump was running in the range of 0.1 μl/min to 100 μl/min (total volume rate 0.3 μl/min to 300 μl/min for all three inputs). For consistency, an average fluid velocity in the array (v_{avg}) is used to represent all simulation and experimental results, where v_{avg} is defined as

This article is copyrighted as indicated in the article. Reuse of AIP content is subject to the terms at: http://scitation.aip.org/termsconditions. Downloaded to IP: 128.112.141.27 On: Wed, 09 Sep 2015 13:48:43

$$v_{avg} = \frac{L_{tot}}{\tau} = \frac{L_{tot}F}{V_{tot}}, \tag{1}$$

where $L_{tot} = l_1 + l_2 = 3$ cm is the total length of the DLD array, $\tau = V_{tot}/F$ is the average residence time for the fluid to flow through the DLD array, F is the volume flow rate, the syringe pump, $V_{tot} = L_{tot}W_{tot}H\theta$ is the total fluid volume of the DLD array, $W_{tot} = 600\,\mu$m and $H = 120\,\mu$m are the total width and the depth of the DLD array, respectively, and $\theta = 1 - \pi(d/2)^2/(g+d)^2 \approx 0.80$ is the "void fraction," i.e., the fraction of the array volume filled with fluid (i.e., excluding the posts). For total volume rate ranging from 0.3 μl/min to 300 μl/min, the average fluid velocity ranges from 86 μm/s to 8.6 cm/s.

Preparation of experiment samples

The running buffer consisted of 150 mM NaCl at pH 7.2 containing 0.09% NaN3, 1% BSA, and 7 mM EDTA. 40 μM D-Phenylalanyl-prolyl-arginyl Chloromethyl Ketone (PPACK) could be added to the running buffer to further reduce on-chip clogging for long time device usage (>30 min).[13] Venous EDTA-anticoagulated blood (purchased from Interstate Blood Bank, Inc., Memphis, TN, USA) was diluted 1:3 with the running buffer as the sample solution. The diluted blood was then used directly as the sample stream input, with no centrifugation or lysis steps. The staining solution (the treatment stream input) was 20 μg/l R6G in the running buffer.

Modelling of the diffusion of the treatment chemical

The diffusion of the treatment chemical in the x-direction, defined as perpendicular to the average fluid flow direction (y-direction, see Fig. 2(a)), is critical issue for our work, since it will cause the contamination of the "washed" product output by the treatment chemical. There

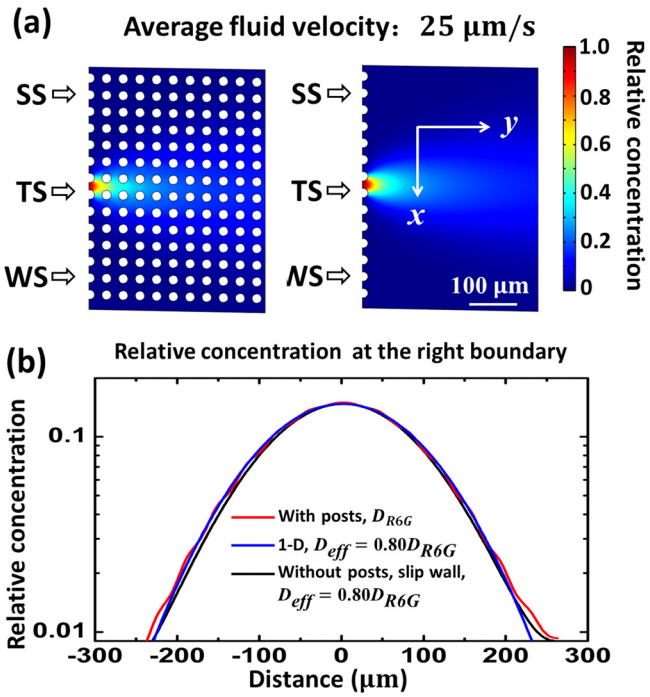

FIG. 2. COMSOL simulations of relative concentration in channels with and without posts. SS: sample input stream, TS: treatment input stream, and WS: washing input stream. Post and gap are about 18 μm. (a) Relative concentration distribution and (b) relative concentration profile at the right boundary along x-direction at average fluid velocity of 25 μm/s. "With posts" and "without posts" refer to COMSOL results using D_{R6G} and $D_{eff} = 0.80D_{R6G}$, respectively. "1-D" refers to a 1-D numerical solution using the same D_{eff}.

This article is copyrighted as indicated in the article. Reuse of AIP content is subject to the terms at: http://scitation.aip.org/termsconditions. Downloaded to IP: 128.112.141.27 On: Wed, 09 Sep 2015 13:48:43

are two major factors that may complicate such diffusion in the devices described in this paper: (1) Taylor-Aris dispersion and (2) the effect of the posts' boundaries. Taylor-Aris dispersion along the fluid flow direction occurs because different streamlines in microstructures can move at different speeds. However, the average flow is along the y-direction in the DLD array. There is no net fluid flow in the x-direction and the local x-direction flow has very low fluid velocity.[11] Thus, classic Taylor-Aris dispersion can be effectively neglected in the x-direction.[14]

The posts can suppress long-range diffusion of the treatment chemical through geometric confinement. Stochastically, for diffusion over a length scale greater than that of the post gap and gap periodicity, the diffusion of the treatment chemical in the post array can be modelled as a diffusion process with an effective diffusion constant D_{eff} in a structure without posts. When the size of the diffusing species is less than 0.1 that of the gap spacing, this D_{eff} has been measured in micropost arrays to be $\theta \cdot D_o$, where D_o is the diffusion constant without posts.[15] These criteria are valid for our experiments, where the size of the R6G molecule is about 1.6 nm (Ref. 16) versus our post spacing of 18 μm. Given $\theta \approx 0.80$ in our experiments, we assume D_{eff} for R6G is equal to $0.80 \cdot D_{R6G}$.

To validate this effective diffusion constant, we modelled diffusion (using COMSOL numerical modelling software) from a central stream with uniform chemical concentration entering a DLD array as used in our experimental work (post diameter and gap are 18 μ m, with tilt angle $\epsilon = 1.36^{\circ}$) over one central gap of 18 μ m. The diffusion was modelled in 2-D over an array length of only 378 μm due to practical grid limitations of COMSOL. The central stream was surrounded on top and bottom by buffer streams (chemical concentration of zero) at the input with the same flow rate per unit width. The diffusion constant of the treatment chemical is set to be $4 \times 10^{-10}\,\mathrm{m}^2/\mathrm{s}$ (the diffusion constant of R6G, D_{R6G}, which is later utilized in experiments). The figure at the left in Fig. 2(a) shows the simulated contour plot of the relative concentration (the ratio of the concentration of the treatment chemical to that in the input chemical stream) in a part of the DLD array with average fluid velocity of 25 μm/s. The average time τ for fluid to flow through the modelled volume was 15.1 s.

The relative concentration profile at the right boundary along the x-direction of simulation with posts (378 μm after the input) is drawn in Fig. 2(b) with a red solid line. To extract an effective long-range diffusion constant, reflecting the effects of confinement, this curve was then fit with a 1-D numerical solution to the diffusion equation for the same initial profile, time $\tau = 15.1$ s, neglecting the effect of the posts, with D_{eff} as an adjustable parameter. This is shown as a blue solid line in Fig. 2(b): $D_{eff} = 3.2 \times 10^{-10}\mathrm{m}^2/\mathrm{s}$ was found to give the best fit. Because the diffusion length $L_D = \sqrt{D_{eff}\tau} \approx 69.6\,\mu$m is well over the array period, D_{eff} should be valid for modelling long range diffusion. Note that the D_{eff}/D_{R6G} ratio of 0.80 is equal to the void fraction, as predicted above.

For modelling diffusion from the central treatment stream to the output channel in our actual devices, we use COMSOL to incorporate the blocking effects of the separator and outer walls. However, the complete post microstructure cannot be included because of grid size limitations, so we model the device without posts with the D_{eff} extracted above. We also increase the input flow rate by 20%, to compensate for the zero void fraction to give the same residence time and average fluid velocity as with posts. Because the flow rate in all gaps across the flow stream in the device array is the same, in the simulations with no posts we also use a "slip" wall boundary condition, so that the flow rate across the entire modelled region is the same. Figs. 2(a) and 2(b) also demonstrate the results of this simulation, showing good profile agreement over long distance with the modelling using the complete microstructure. Therefore, for the rest of this paper, to model diffusion to the product output, COMSOL was used in a structure with no posts using $D_{eff} = 0.80 D_{R6G}$.

RESULTS AND DISCUSSION

Diffusion of treatment chemical to the product output

Simulation results of the relative concentration of the treatment chemical for devices with no separator wall, one separator wall, and two separator walls using COMSOL are shown in

This article is copyrighted as indicated in the article. Reuse of AIP content is subject to the terms at: http://scitation.aip.org/termsconditions. Downloaded to IP: 128.112.141.27 On: Wed, 09 Sep 2015 13:48:43

Fig. 3. The relative concentration of the treatment chemical is shown at the chip input, middle of the chip, and the chip output. The reduction of treatment chemical contamination at the product output brought by the first and second separator walls can be seen clearly from these simulation results. At average fluid velocity of 100 μm/s for the design with only the first separator wall (Fig. 3(a)), the treatment chemical is blocked by the first separator wall, but still has enough time in the last section of the chip to diffuse unboundedly across the entire flow path, so that the 1-wall design is little better than the conventional no wall design. The contamination in the product output is calculated as the average relative concentration of the treatment chemical over the 60 μm-wide product output channel. By implementing the second separator wall, this relative contamination can be reduced from 0.31 down to 0.14. With the average fluid velocity of 1 cm/s (Fig. 3(b)), the diffusion time is reduced, but the conventional design still has an output contamination of relative concentration about 0.081. The output contamination is suppressed ~4-fold with the first separator wall design and can be further reduced utilizing two separator walls down to 0.008, a 10-fold improvement over the design without separator walls.

We also experimentally measured the diffusion of R6G in the fabricated arrays without and with separator walls by quantitative fluorescence microscopy. Similar to the simulation results, the output contamination due to the diffusion of R6G was evaluated by the average relative R6G concentration entering the product output. The relative R6G concentration is defined as the ratio of the fluorescence intensity of R6G to that of the treatment stream input, as the fluorescence intensity of R6G has a linear relation to its concentration at low concentration.[17] Figs. 4(a) and 4(b) display the fluorescence images of the input, middle, output region of DLD arrays without and with separator walls of same length, but with otherwise identical dimensions. At average fluid velocity 0.86 mm/s, the contamination at the product output almost reaches saturated level about 0.3 in the conventional DLD array (Fig. 4(a)). In the wall-separated array, the presence of separator walls leads to a 3 fold output contamination reduction down to about 0.1 (Fig. 4(b)).

The experiment results at different fluid velocities agree well with the numerical simulation, as shown in Fig. 4(c). The output contamination depends on how fast the diffusion of the treatment chemical occurs compared to the rate at which the fluid moves through the device, classically characterized by Peclet number. For a device without separator walls, a critical velocity (v_c) will be the one which the diffusion length $L_D = \sqrt{D_{eff}\tau}$ is equal to the distance from the treatment stream to the product output location, which is w_W, the width of the washing stream, where $\tau \approx L_{tot}/v_c$ is the time the fluid is in the device. Thus, a critical fluid velocity can be written as

$$v_c = \frac{D_{eff} L_{tot}}{w_W^2}. \tag{2}$$

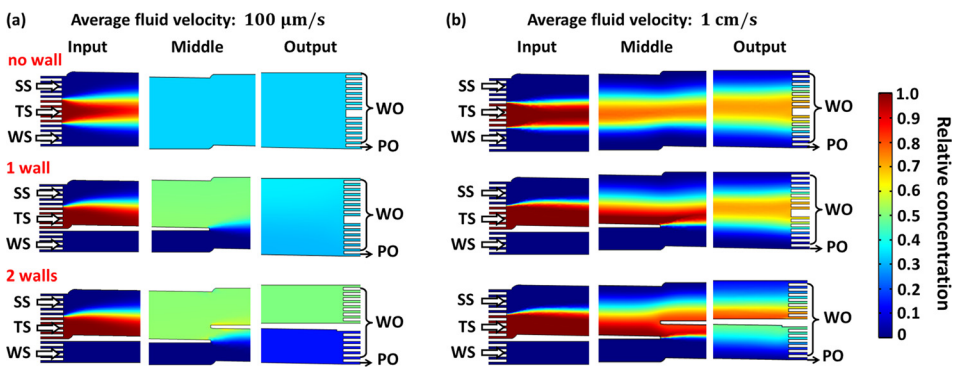

FIG. 3. COMSOL simulations of relative concentration across devices with no separator wall, one separator wall, and two separator walls at average fluid velocity 100 μm/s and 1 cm/s. WO: waste output and PO: product output. Each condition shows the input, middle, and output regions (0.8 mm long) of the devices. For 100 μm/s (1 cm/s), the relative output contamination is 0.33 (0.081), 0.31 (0.022), and 0.14 (0.008) with no, 1, and 2 separator walls, respectively. The output contamination of the treatment chemical can be reduced effectively with the separator wall design.

This article is copyrighted as indicated in the article. Reuse of AIP content is subject to the terms at: http://scitation.aip.org/termsconditions. Downloaded to IP: 128.112.141.27 On: Wed, 09 Sep 2015 13:48:43

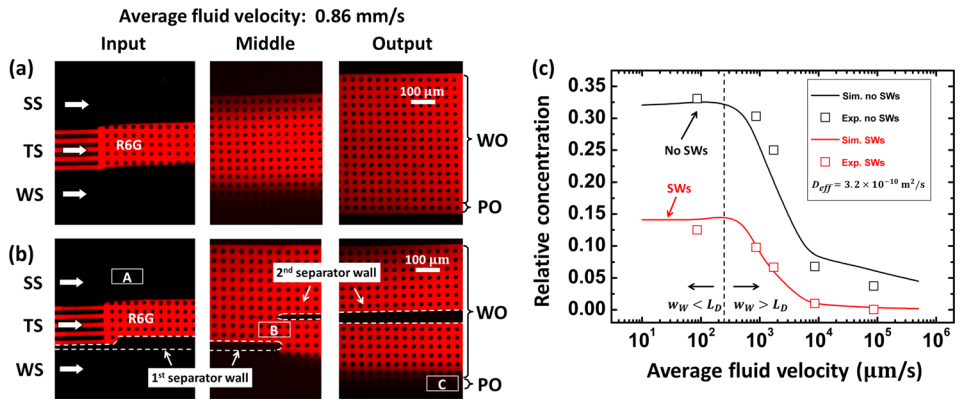

FIG. 4. Fluorescent images of R6G flowing in the treatment stream of (a) conventional DLD array and (b) DLD array with two separator walls, showing clear reduction of contamination at the product output. The average fluid velocity is 0.86 mm/s. (c) Experimental and COMSOL simulation results of relative concentration versus average fluid velocity for both conventional (black) and wall-separated (red) DLD arrays. The open squares are experiment results measured as the ratio of the fluorescence intensity at the product output to that of the treatment stream input. The solid lines are the COMSOL simulation results. A dotted black line is drawn in (c) to point out the critical fluid velocity of 240 μm/s for the conventional design. R6G concentration is 20 μg/ml.

For a conventional DLD array, a vertical black dotted line in Fig. 4(c) indicates this critical fluid velocity of 240 μm/s. At fluid velocity lower than v_c, $w_W < L_D$ and the contamination reaches a plateau. At fluid velocity higher than v_c, $w_W > L_D$ and the contamination drops.

For the "wall-separated" DLD array, the time for diffusion in the device is reduced from $(l_1 + l_2)/v$ to l_2/v, where v is the average fluid velocity, and the second separator wall in the latter region of the device further prevents some treatment chemical from being able to move to the output. The improvement in the output contamination reduction is 3 to 10 fold, depending on the fluid velocity (Fig. 4(c)). For example, from the experimental results, at average fluid velocity 8.6 mm/s, the R6G concentration in the product output channel can be reduced from 0.07 without separator walls to only 0.01 with the implementation of separator walls.

Incubation time vs. output contamination

The minimum incubation time is a key factor of on-chip cell processing and preparation applications. We now estimate the minimum incubation time in the "wall-separated" DLD array. The cells flowing into the device at the topmost boundary will experience the minimum incubation time (P1 in Fig. 1(a)). This minimum incubation time t_{min} in the wall-separated DLD array can be estimated as

$$t_{min} \approx \frac{w_T}{\epsilon v_{cell,DLD}} + \frac{\epsilon l_1 - w_T - w_S}{\epsilon v_{max,post-wall}}, \tag{3}$$

where w_T and w_S are the widths of treatment stream and sample stream, respectively, $v_{cell,DLD}$ is the cell velocity in the DLD array, and $v_{max,post-wall}$ is the maximum fluid velocity between the posts and the confining wall. When the target cells flow in the DLD array, their velocity will change periodically from fast in the gaps to slow in the open regions. To estimate the minimum incubation time, we conservatively use the cell fluid velocity in post gaps. The average fluid velocity ($v_{avg,post-post}$) in post gaps is about 1.62 times the average fluid velocity in the DLD array for the proposed geometry. The target cells which are above the critical size and thus are "bumped" by the posts at every column of obstacles will move alongside the posts as they follow the tilt angle (target cell in Fig. 1(b)). Assuming the large target cell moves at the fluid velocity of the streamline where the cell center is and a parabolic flow profile, the cell's velocity is $v_{cell,DLD} \approx 4v_{max,post-post}(r_{cell}/g - r_{cell}^2/g^2)$, where r_{cell} is the radius of the target cells

This article is copyrighted as indicated in the article. Reuse of AIP content is subject to the terms at: http://scitation.aip.org/termsconditions. Downloaded to IP: 128.112.141.27 On: Wed, 09 Sep 2015 13:48:43

(r_{cell} of 3.5 μm is assumed for leukocytes), and $v_{max,post-post} = 3/2 v_{avg,post-post}$ is the maximum fluid velocity in the post gaps.[11]

The second term of Eq. (3) is the additional incubation time gained by implementing the first separator wall. The incubation time can be increased by increasing the total length of the first separator wall without any penalty of the contamination of the treatment chemical in the product output. As the target cell further moves along the first separator wall, it will be driven to an equilibrium position where the wall effect lift force and the shear gradient lift force balance.[18] From experimental observations, the equilibrium position of leukocytes is close to the middle of the gap between the wall and the posts, where the fluid velocity reaches an average maximum ($v_{max,post-wall}$) (Fig. 1(b)). By design, the average $v_{max,post-wall}$ is approximately equal to $v_{max,post-post}$ discussed above.

Experimental and COMSOL simulation results of the relative output contamination versus calculated minimum incubation time according to Eq. (3) for both conventional (black) and "wall-separated" (red) DLD arrays are shown in Fig. 5. For high fluid velocity, both incubation time and output contamination are low. They both rise as the fluid velocity is decreased. For a leukocyte staining test, average fluid velocity of 1.7 mm/s is selected (pointed out by the red dash lines) as an experimental on-chip leukocyte staining condition, with ~4 s minimum incubation time and 0.067 product output contamination. As can be seen from the later experiments, leukocytes can be stained with recognizable fluorescence intensity compared to very low background intensity of contamination at this condition.

We then used the wall-separated device to demonstrate on-chip staining and washing of leukocytes with R6G, using diluted whole blood as the sample stream input. R6G diffuses into the cells and attaches to their mitochondria.[10] The array separates the leukocytes out of the sample stream and then directs them into the treatment and the subsequential washing streams. The critical size (D_c) is about 6 μm in the proposed DLD array measured by fluorescent beads of different sizes, which is below the size of most leukocytes. The diameter of erythrocytes is about 6–8 μm. However, since their distinctive biconcave shape, they align to the fluid flow to behave as small particles and are not displaced in the array, thus following the average fluid direction.[19] Moreover, the size of the other content (platelets, proteins, etc.) of blood is mostly smaller than 6 μm, so that only leukocytes are harvested from the sample stream. Fluorescent microscopy was used to track the paths and staining of the cells (Fig. 6). In the input region, no fluorescent leukocytes or other cells could be seen as the cells were not yet labeled (movie M1 in the supplementary material[20] from region "A" of Fig. 4(b)). The

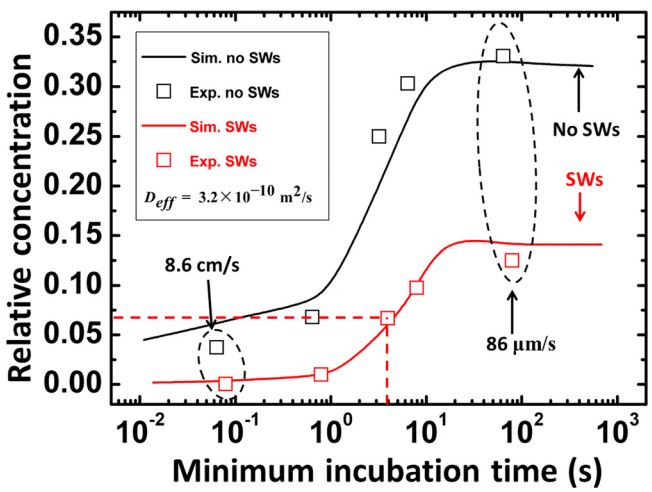

FIG. 5. Experimental and COMSOL simulation results of relative concentration versus calculated minimum incubation time for both conventional (black) and wall-separated (red) DLD arrays, achieved by varying the average fluid velocity. The open squares are experimental results and the solid lines are the COMSOL simulation results. The condition for the two-separator wall design of an average fluid velocity of 1.7 mm/s with ~4 s minimum incubation time and 0.067 product output contamination (indicated by red dotted lines) was selected for subsequential staining tests.

This article is copyrighted as indicated in the article. Reuse of AIP content is subject to the terms at: http://scitation.aip.org/termsconditions. Downloaded to IP: 128.112.141.27 On: Wed, 09 Sep 2015 13:48:43

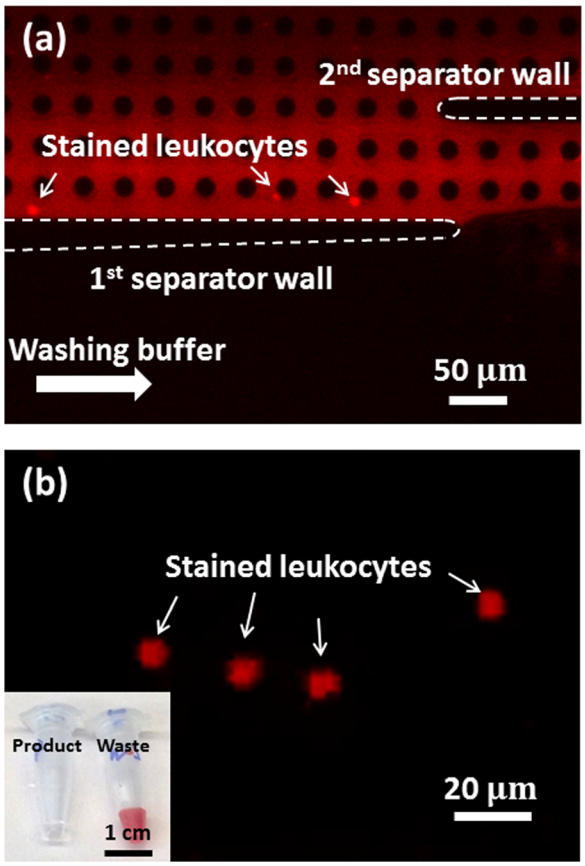

FIG. 6. Fluorescent images of on-chip leukocyte staining with R6G with wall-separated DLD arrays using diluted human blood as the input, without any centrifugation or lysis. The average fluid velocity is 1.7 mm/s. View (a) shows middle region of the wall-separated DLD array where the leukocytes are passing through the R6G stream and close to entering into the washing stream (region "B" in Fig. 3(b) and movie M2 in the supplementary material).[20] View (b) shows labeled leukocytes in the output channel with negligible fluorescence background. The inset of (b) shows vials of collected product and waste outputs, showing low red blood cell level in the product.

leukocytes were then concentrated and incubated along the first separator wall in the middle region of the wall-separated DLD array (Fig. 5(a) and movie M2 in the supplementary material[20] from region "B" of Fig. 3(b)). Finally, the labeled leukocytes are collected at the product output (movie M3 in the supplementary material[20] from region "C" of Fig. 4(b)) and clearly visible (Fig. 5(b)). The inset of Fig. 5(b) shows the product output and waste output vails from one experiment of 200 μl diluted blood. The notable color difference suggests a good separation of leukocytes from erythrocytes. In the fluorescence image of the product output stream, little fluorescence background could be found, indicating a good staining by R6G and low contamination of unreacted R6G in the product output.

CONCLUSION

We presented a wall-separated DLD array for integrated on-chip cell harvesting, chemical processing, and washing. The "wall-separated" design greatly improves the trade-off between long chemical treatment times and low output contamination at low fluid velocity, enabling both (i) increased incubation time and (ii) less contamination of treatment chemical in the product output. We demonstrated that leukocytes can be separated from the whole blood, stained by R6G, and washed in a single device without any pre-processing of the blood or manual handling between steps. The device should be applicable to other on-chip processing and washing steps such as labelling with monoclonal antibodies, fixation/permeabilization, and other novel applications.

This article is copyrighted as indicated in the article. Reuse of AIP content is subject to the terms at: http://scitation.aip.org/termsconditions. Downloaded to IP: 128.112.141.27 On: Wed, 09 Sep 2015 13:48:43

ACKNOWLEDGMENTS

This work was supported by GPB Inc. and by a NIH Phase I STTR grant (Grant No. 2R41CA174121).

[1]O. Kolar and W. Zeman, Arch. Neurol. **18**, 44–51 (1968).
[2]M. A. McClain, C. T. Culbertson, S. C. Jacobson, N. L. Allbritton, C. E. Sims, and J. M. Ramsey, Anal. Chem. **75**, 5646–5655 (2003).
[3]J. Nguyen, Y. Wei, Y. Zheng, C. Wang, and Y. Sun, Lab Chip **15**, 1533–1544 (2015).
[4]A. Mach, J. H. Kim, A. Arshi, S. C. Hur, and D. Di Carlo, Lab Chip **11**, 2827–2834 (2011).
[5]A. P. Tan, J. S. Dudani, A. Arshi, R. J. Lee, H. T. K. Tse, D. R. Gossett, and D. Di Carlo, Lab Chip **14**, 522–531 (2014).
[6]K. J. Morton, K. Loutherback, D. W. Inglis, O. K. Tsui, J. C. Sturm, S. Y. Chou, and R. H. Austin, Lab Chip **8**, 1448–1453 (2008).
[7]J. A. Davis, D. W. Inglis, K. J. Morton, D. A. Lawrence, L. R. Huang, S. Y. Chou, J. C. Sturm, and R. H. Austin, Proc. Natl. Acad. Sci. U. S. A. **103**, 14779–14784 (2006).
[8]D. W. Inglis, J. A. Davis, T. J. Zieziulewicz, D. A. Lawrence, R. H. Austin, and J. C. Sturm, J. Immunol. Methods **329**, 151–156 (2008).
[9]A. R. L. Gear, J. Biol. Chem. **249**(11), 3628–3637 (1974); available at http://www.jbc.org/content/249/11/3628.abstract.
[10]L. K. Tamm, Biochemistry **27**, 1450–1457 (1988).
[11]D. W. Inglis, J. A. Davis, R. H. Austin, and J. C. Sturm, Lab Chip **6**, 655–658 (2006).
[12]D. W. Inglis, Appl. Phys. Lett. **94**, 013510 (2009).
[13]J. D'Silva, R. H. Austin, and J. C. Sturm, Lab Chip **15**, 2240–2247 (2015).
[14]I. Ippolito, E. J. Hinch, G. Daccord, and J. P. Hulin, Phys. Fluids A **5**, 1952–1962 (1993).
[15]K. He, F. B. Khorasani, S. T. Retterer, D. K. Thomas, J. C. Conrad, and R. Krishnamoorti, ACS Nano **7**, 5122–5130 (2013).
[16]I. I. Vlasov, A. A. Shiryaev, T. Rendler, S. Steinert, S.-Y. Lee, D. Antonov, M. Voros, F. Jelezko, A. V. Fisenko, L. F. Semjonova, J. Biskupek, U. Kaiser, O. I. Lebedev, I. Sildos, P. R. Hemmer, V. I. Konov, A. Gali, and J. Wrachtrup, Nat. Nanotechnol. **9**, 54–58 (2014).
[17]F. M. Zehentbauer, C. Moretto, R. Stephen, T. Thevar, J. R. Gilchrist, D. Pokrajac, K. L. Richard, and J. Kiefer, Spectrochim. Acta A **121**, 147–151 (2014).
[18]L. Zeng, S. Balachandar, and P. Fischer, J. Fluid Mech. **536**, 1–25 (2005).
[19]K. K. Zeming, S. Ranjan, and Y. Zhang, Nat. Commun. **4**, 1625 (2013).
[20]See supplementary material at http://dx.doi.org/10.1063/1.4930863 for supplementary movies and text.

This article is copyrighted as indicated in the article. Reuse of AIP content is subject to the terms at: http://scitation.aip.org/termsconditions. Downloaded to IP: 128.112.141.27 On: Wed, 09 Sep 2015 13:48:43